Journal of Pharmaceutical and Biomedical Analysis 137 (2017) 60–69

Contents lists available at ScienceDirect

Journal of Pharmaceutical and Biomedical Analysis

journal homepage: www.elsevier.com/locate/jpba

Separation of antibody drug conjugate species by RPLC: A generic method development approach

Szabolcs Fekete[a,*], Imre Molnár[b], Davy Guillarme[a]

[a] School of Pharmaceutical Sciences, University of Geneva, University of Lausanne, CMU – Rue Michel Servet, 1, 1211 Geneva 4, Switzerland
[b] Molnár-Institute for Applied Chromatography, Schneeglöckchen Strasse 47, 10407 Berlin, Germany

ARTICLE INFO

Article history:
Received 7 December 2016
Received in revised form 5 January 2017
Accepted 6 January 2017
Available online 11 January 2017

Keywords:
Retention modelling
Antibody drug conjugate
Brentuximab vedotin
Method development
DryLab
Reversed phase liquid chromatography

ABSTRACT

This study reports the use of modelling software for the successful method development of IgG1 cysteine conjugated antibody drug conjugate (ADC) in RPLC. The goal of such a method is to be able to calculate the average drug to antibody ratio (DAR) of and ADC product. A generic method development strategy was proposed including the optimization of mobile phase temperature, gradient profile and mobile phase ternary composition. For the first time, a 3D retention modelling was presented for large therapeutic protein. Based on a limited number of preliminary experiments, a fast and efficient separation of the DAR species of a commercial ADC sample, namely brentuximab vedotin, was achieved. The prediction offered by the retention model was found to be highly reliable, with an average error of retention time prediction always lower than 0.5% using a 2D or 3D retention models. For routine purpose, four to six initial experiments were required to build the 2D retention models, while 12 experiments were recommended to create the 3D model. At the end, RPLC can therefore be considered as a good method for estimating the average DAR of an ADC, based on the observed peak area ratios of RPLC chromatogram of the reduced ADC sample.

1. Introduction

Antibody drug conjugates (ADCs) are chemotherapeutics constituted of a cytotoxic chemical drug linked covalently – via peptide linker – to a monoclonal antibody (mAb) [1]. They are used for the treatment of cancer by combining the proven antigen-specific selectivity and activity of mAbs with the potency of highly cytotoxic small molecules [2]. Drug conjugation can be achieved via reactions at different amino acid residues such as at lysine side chains amines (lysine conjugation), at cysteine thiol groups after reduction of the interchain disulfide bonds (cysteine conjugation), or at engineered cysteine residues at specific sites on a mAb [3,4]. The addition of the drugs results in a heterogeneous population of ADCs that differ in the number of drugs per antibody, and this mixture can be described by an average drug to antibody ratio (DAR) [4]. Structurally, immunoglobulin G1 (IgG1) mAbs contain four interchain disulphide bridges. Among those, two are located in the hinge region and connect the two heavy chains (H) while the other two connect the H and light chain (L). Therefore, a cysteine linked IgG1 ADC is composed of a heterogeneous mixture of 0, 2, 4, 6 or 8 drug conjugations [5]. An odd number of conjugated drugs on an ADC is typical indicative of degradation [6,7]. In this study, we focus only on a commercially available cysteine linked IgG1 ADC, namely brentuximab vedotin.

One of the most important critical quality attributes (CQA) of an ADC is the average DAR, since it determines the amount of "payload" that can be delivered to a tumor cell and can affect efficacy and safety [3]. A variety of analytical methods have been used to measure the average DAR, including UV–vis spectroscopic, liquid chromatographic, and native mass spectrometric methods [4,8–19]. Among liquid chromatographic methods, hydrophobic interaction chromatography (HIC) and reversed phase chromatography (RPLC) are routinely used. The former approach separates the intact DAR species under non-denaturating conditions, while RPLC is mostly used to separate the DAR species of reduced ADC sample related to the H or L chains as L0, L1 and H0, H1, H2 and H3 species.

In addition to information about the average DAR, multiple methods have been applied to analyze the distribution of drug linked forms and their positional isomers. This is again an important characteristic because different forms may have different pharmacokinetic and toxicological properties [3,16]. A number of methods for this task are based on the use of mass spectrometry (MS) [20–23]. The separation of intact DARs in HIC also allows the isolation of pure species and permits further characterization (e.g.

* Corresponding author.
E-mail address: szabolcs.fekete@unige.ch (S. Fekete).

http://dx.doi.org/10.1016/j.jpba.2017.01.013
0731-7085/

by capillary electrophoresis-sodium dodecyl sulphate and capillary iso-electric focusing (CE-SDS, cIEF) or cell based bioassay) [3,5]. The complete characterization of ADC DAR positional isomers can also be performed on-line, by peptide mapping LC–MS or two dimensional (HIC x RPLC)-MS analysis of the native ADC [6,7,24,25]. In addition to average DAR, DAR distribution and positional isomer analysis, a number of complementary methods can be applied for further characterization of ADCs to determine residual free drugs, size variants or charge variants [25].

As mentioned earlier, RPLC is mostly used to separate the DAR species of reduced ADC related to H and L, but can also be applied on the native ADC to separate L, H, HH, HL and HHL fragments. The latter one can be useful, as a second dimension separation prior to MS. In the literature, only "historical" methods are reported, using a mobile phase containing 0.1% trifluoroacetic-acid (TFA), an acetonitrile gradient and elevated temperature of 70–80 °C. However, nothing is reported about systematic method development, optimization procedure or retention behavior. In this study, we offer a possible generic method development approach for IgG1 cysteine conjugations. Both 2D and 3D retention models are discussed. The impact of temperature and mobile phase ternary composition was also studied. Finally, four, six and twelve experiments based designs were suggested for routine purposes. This new approach allows a fast and accurate systematic method development for the efficient separation of ADC DAR species and fragments.

2. Experimental

2.1. Chemicals and columns

Water was obtained from a Milli-Q Purification System from Millipore (Bedford, MA, USA).

Acetonitrile (ACN) and methanol (MeOH) were ULC–MS grade and purchased from Biosolve (Valkenswaald, Netherlands). Dithiothreitol (DTT, ≥99.0%) and trifluoroacetic acid (TFA, 99%) were purchased from Sigma–Aldrich (Buchs, Switzerland).

Brentuximab vedotin as therapeutic monoclonal antibody drug conjugate (IgG1 cysteine linked ADC) was kindly provided by the Center of Immunology Pierre Fabre (Saint-Julien en Genevois, France).

The AdvanceBio RP-mAb C4 (3.5 μm, 150 mm × 2.1 mm, 450 Å) column was purchased from Agilent (USA).

2.2. Equipment and software

Measurements were performed using a Waters Acquity UPLC™ I-Class system equipped with a binary solvent delivery pump (maximum flow rate of 2 mL/min and upper pressure limit of 1200 bar), an auto-sampler and UV detector. The system includes a flow through needle (FTN) injection system with 15 μL needle and a 0.5 μL UV flow-cell. The overall extra-column volume (V_{ext}) was about 7.5 μL as measured from the injection seat of the auto-sampler to the detector cell. The dwell volume was measured as V_d = 0.09 mL.

Data acquisition and instrument control were performed by Empower Pro 3 software (Waters). Calculations and data transferring were achieved with Excel (Microsoft). Retention and resolution modelling was performed with DryLab® 4 software (Molnár-Institute, Berlin, Germany).

2.3. Mobile phase composition and sample preparation

For the gradient separation of ADC DARs and its fragments, the mobile phase "A" consisted of 0.1% TFA in water, whereas the mobile phase "B" was 0.1% TFA in organic solvent having different possible compositions of acetonitrile and methanol.

Native brentuximab vedotin was injected as received (5 mg/mL) using low volume insert vials.

Reduced brentuximab vedotin sample was prepared by the addition of DTT solution (10 mM) and incubation at 30 °C for 60 min. The ADC was completely converted into the light and heavy chain components. Then, sample was injected from low volume insert vial.

2.4. Investigation of retention properties of ADC species (preliminary studies)

Native brentuximab vedotin was eluted in RPLC mode using linear gradients. The effect of the gradient profile, temperature and organic modifier on the retention and selectivity of ADC species was studied. Detection was carried out at 280 nm, and 1 μL sample was injected.

First, the effect of gradient steepness (gradient time, t_G) on retention and selectivity was evaluated. A generic linear gradient, starting from 25% to 50% B was applied at a flow rate of 0.3 mL/min. For mobile phase B, acetonitrile was used as organic modifier and the experiments were performed at T = 90 °C. In our previous study, the validity of linear solvent strength model (LSS) was proved for mAbs and subunits in the practically relevant design space (DS) [26]. The gradient time was varied as t_G = 6, 12 and 18 min. The observed apparent (or gradient) retention factors (k_{app}) were plotted against t_G and the change in selectivity (elution order) was followed.

Based on previous experiments, high temperature seemed to be mandatory for correct peak shape and recovery [27]. Therefore, all the experiments were performed at mobile phase temperature of T ≥ 70 °C. Short gradient runs (t_G = 6 min) were carried out at 70, 75, 80, 85 and 90 °C (up to the upper temperature limit of the column). Our purpose was to illustrate the effect of temperature on the retention and recovery. Plots of log k_{app} *vs.* 1/T and recovery *vs.* T were made. For the estimation of recovery, peak area values were normalized to the ones observed at the highest temperature (90 °C).

At last, the impact of the organic modifier was studied by running gradients with mixtures of acetonitrile and methanol. Aprotic and protic solvents may have an impact on the solvation of ADC species and can interact in different ways with the proteins and also with the residual acidic silanols of the silica based stationary phase. Therefore, differences in retention and selectivity were expected. Ternary mobile phases were prepared using water, acetonitrile and methanol. The ternary composition (*tC*) of mobile phase B was set as 0, 20, 40 and 50% MeOH in ACN. Since MeOH has a lower eluent strength than ACN, the gradients were run in an extended%B range (30–80%B), to elute all the species with all mobile phase compositions. The experiments were performed at T = 90 °C, and t_G = 6 min. Higher than 50% MeOH content resulted in unacceptable recovery and too high retention.

2.5. Systematic method optimization

Snyder et al. recommended initial basic runs for multifactorial experimental designs already in the 90's [28]. A general approach is to simultaneously model the effect of temperature and gradient steepness (t_G) on selectivity with a previously selected RPLC column [29,30]. Then, with the help of resolution maps generated by modelling software – which show the critical resolution of the peaks to be separated [31] – the gradient program and column temperature can be rapidly and efficiently optimized. Today – thanks to new developments of modelling software – it is also possible to simultaneously optimize three method variables. Beside temperature and gradient steepness, ternary mobile phase composition or mobile phase pH are often selected as third variable [32–34]. Since

neither ternary composition nor mobile phase pH impact retention in a linear fashion, their effect have to be measured at least at three levels. The dependence of retention on both t_G and T can be transferred to linear relationships and therefore necessitate only

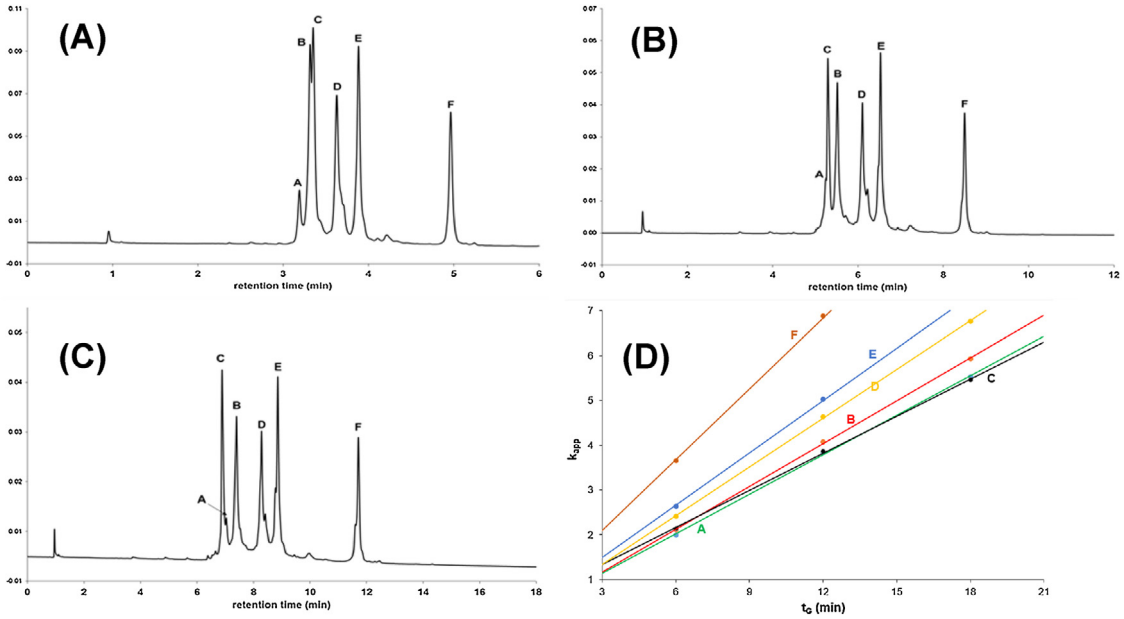

Fig. 1. The impact of gradient steepness on selectivity. Column: Agilent Advance BioMAb RP C4. Mobile phase "A": 0.1% TFA in water, "B": 0.1% TFA in acetonitrile. Flow rate: 0.3 mL/min, gradient: 25–50% B (in 6 min (A), 12 min (B) and 18 min (C)), temperature: 90 °C, injected volume: 1 μL, detection at 280 nm. Panel D shows the dependence of k_{app} on the gradient time. Sample: Brentuximab vedotin.

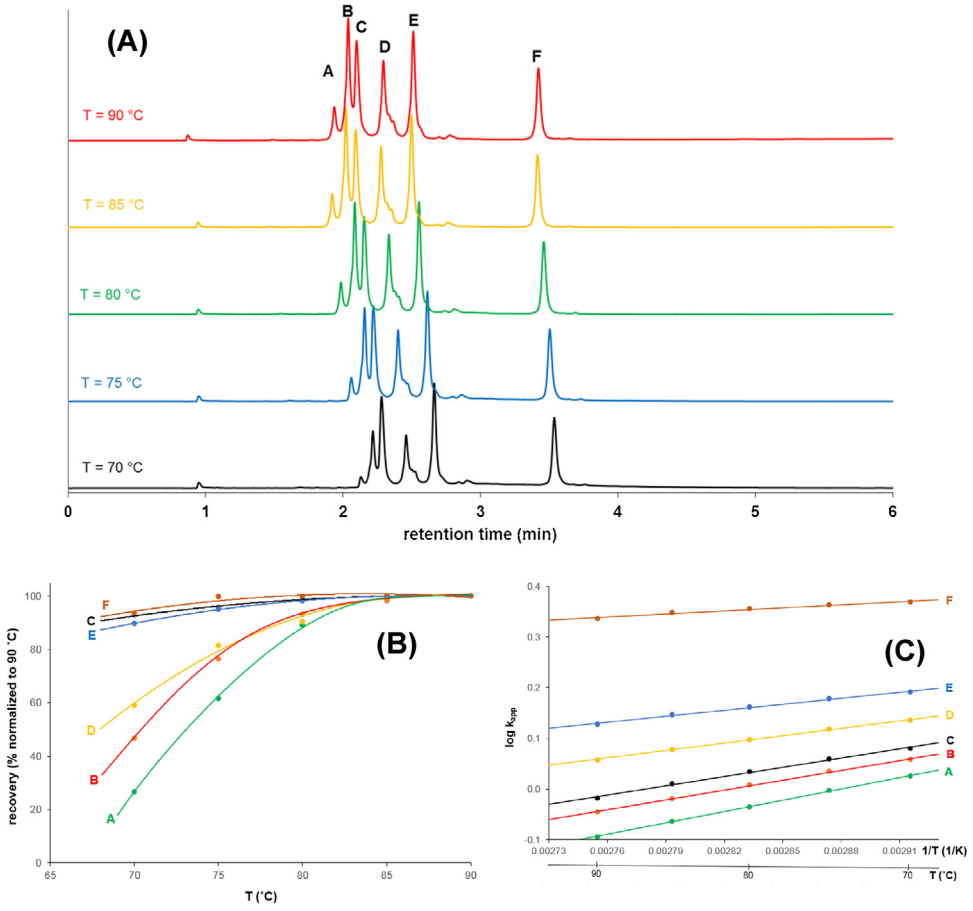

Fig. 2. The impact of mobile phase temperature on the retention times (A), peak area (recovery) (B) and retention factor (C) of different ADC species. Column: Agilent Advance BioMAb RP C4. Mobile phase "A": 0.1% TFA in water, "B": 0.1% TFA in acetonitrile. Flow rate: 0.3 mL/min, gradient: 30–60% B in 6 min (extended gradient to enable baseline resolution and the measurement of peak areas), temperature: 90 °C, injected volume: 1 μL, detection at 280 nm. Sample: Brentuximab vedotin.

two experiments for one variable to build up an accurate retention model. In our DS, these linear relationships were found to be valid for large ADC species.

In this study, the most information retention model for ADC subunits was found to be a twelve experiments based combined 3D model of $t_G \times T \times tC$. The gradient time was set as $t_{G1} = 10$ min and $t_{G2} = 20$ min, temperature was studied at $T_1 = 75\,^{\circ}C$ and at $T_2 = 90\,^{\circ}C$ while ternary composition was set at $tC_1 = 0\%$, $tC_2 = 10\%$ and $tC_3 = 20\%$ MeOH in ACN. Longer gradients than 20 min were not considered to avoid on column degradation of large ADC species at elevated temperature. The experiments were performed at a flow rate of 0.3 mL/min (25–50% B, linear gradients). The accuracy of retention models were verified in the center point of the DS, namely $t_G = 15$ min, T = 82,5C and $tC = 10\%$ MeOH.

Mobile phase pH was not an important method variable, and 0.1% TFA is commonly added to the mobile phase to have ion-pairs with the positively charged proteins and a pH of around 2 in the mobile phase.

Simplified 2D retention models were also suggested as $t_G \times T$ and $t_G \times tC$. The former one requires four initial experiments, while the latter one needs six experimental runs. These 2D models were built up on the basis of experimental runs performed for the 3D model. For the first 2D model $t_{G1} = 10$ min, $t_{G2} = 20$ min, $T_1 = 75\,^{\circ}C$ and $T_2 = 90\,^{\circ}C$ were considered (with 0% MeOH in mobile phase B). For the second 2D model $t_{G1} = 10$ min, $t_{G2} = 20$ min, $tC_1 = 0\%$, $tC_2 = 10\%$ and $tC_3 = 20\%$ MeOH in ACN were considered at $T = 90\,^{\circ}C$.

Optimal conditions (working points) were determined for both the native and reduced brentuximab vedotin and then the accuracy of retention time prediction was studied. Simulated robustness test was also performed around the working point.

3. Results and discussion

3.1. Preliminary measurements

In RPLC, interaction with the stationary phase is mediated predominantly through hydrophobic interactions between the nonpolar amino acid residues of proteins and the immobilized *n*-alkyl ligands. Solutes are eluted in their order of increasing molecular hydrophobicity. The retention of mAb and ADC species, i.e. large biomolecules is strongly dependent on small changes in the solvent strength and a very small change (<1%) in the organic modifier content could lead to a significant shift in the retention. For this reason, isocratic conditions are impractical, and gradient elution is mandatory. In addition, the peak shape of large molecules is always better in gradient mode compared to isocratic one due to band focusing effects. The LSS model is the widely accepted theory which describes the analyte retention as a function of the volume fraction (Φ) of the eluting B solvent. This model generally well describes the retention of numerous types of analytes including large proteins such as mAbs or mAb sub-units [26].

Fig. 1 shows the impact of t_G on selectivity and k_{app}. Interestingly, the selectivity between some peaks changes drastically with t_G. With a fast gradient ($t_G = 6$ min), the first three peaks elute in the following order: A, B and C. When increasing t_G to 12 min, the elution order of B and C changes. Further increasing t_G (18 min) results in a new elution order, namely C, A and B. Fig. 1D well represents the effect of t_G on selectivity since the fitted curves of k_{app} vs t_G for peaks A, B and C cross each other in the studied range. Moreover, the LSS behavior of the ADC species was also illustrated, since linear trends fit perfectly with the experimental data. These preliminary results suggest that gradient steepness is a very important method variable to optimize ADC separations under RPLC conditions.

The effect of temperature on retention factor is generally expressed by the van't Hoff relationship. When log k_{app} is plotted against 1/T, a linear relationship is expected for regular solutes. However, with large biomolecules, the effect of temperature on retention becomes more complex. Depending on the stability of the secondary structure, the molecules unfold to various extents and hence interact with the stationary phase with various strengths [35]. Due to the different conformation-dependent responses of proteins at elevated temperatures, the change in retention can be very different [36,37]. Another issue related to temperature is the possible thermal degradation of proteins when working at elevated temperature [27]. It was shown for mAbs that analysis time should be kept below 20 min to avoid degradation at 70–90 °C. On the other hand, high temperature is mandatory to limit protein adsorption on the stationary phase. A temperature lower than 70 °C results in unacceptable recovery for most mAbs [38]. Therefore, it is important to work in a limited range in terms of temperature and analysis time. If the analysis time is no longer than 20 min, then, a van't Hoff like behavior is expected between 70 and 90 °C for mAbs and subunits [26]. Fig. 2A shows the observed chromatograms of brentuximab vedotin measured at 70, 75, 80, 85 and 90 °C. As shown in Fig. 2A, the ratio of peak areas of the main peaks (A–F) changes with temperature. The change of peak areas was especially important for peaks A, B and D. As reported in Fig. 2B, only 27, 47 and 59% of peak areas was observed at 70 °C for peaks A, B and D compared to 90 °C. Based on previous studies [6,7], these peaks probably correspond to the naked mAb (and mAb with two drugs on the H in the hinge region), the conjugated light chain (L1) and different HHL species (HHL1 and HHL3). To have at least 50% recovery for all peaks, the temperature should not be set below 75 °C. Fig. 2C confirms the van't Hoff like behavior of these ADC species within the applied temperature range. It is important since it enables to study the effect of temperature on retention only at two levels and simplifies the experiments.

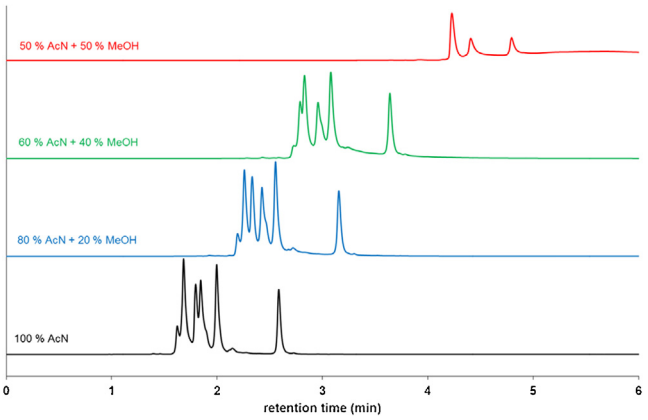

Fig. 3. The impact of mobile phase ternary composition. Column: Agilent Advance BioMAb RP C4. Mobile phase "A": 0.1% TFA in water, "B": 0.1% TFA in acetonitrile and methanol mixture. Flow rate: 0.3 mL/min, gradient: 30–80% B in 6 min (extended gradient to enable eluting all the peaks with 50% MeOH content), temperature: 90 °C, injected volume: 1 μL, detection at 280 nm. Sample: Brentuximab vedotin.

Another interesting variable is the mobile phase ternary composition. Fig. 3 shows the impact of organic modifier nature in mobile phase B. Increasing MeOH *vs.* ACN results in expected increase of retention. In addition, some differences in selectivity were also observed. However, a drawback of using huge MeOH fraction is the non-desired adsorption of the ADC species onto the stationary phase. The sum of peak areas decreases when increasing the MeOH content. At 50% MeOH, only about 30% of total peak area was observed, which is not acceptable. The MeOH fraction of mobile phase B should then, not be larger than 20% to get appropriate recovery for all peaks.

To conclude on the preliminary studies, t_G, T, and tC all seem to be interesting variables to optimize or adjust the separation of ADC

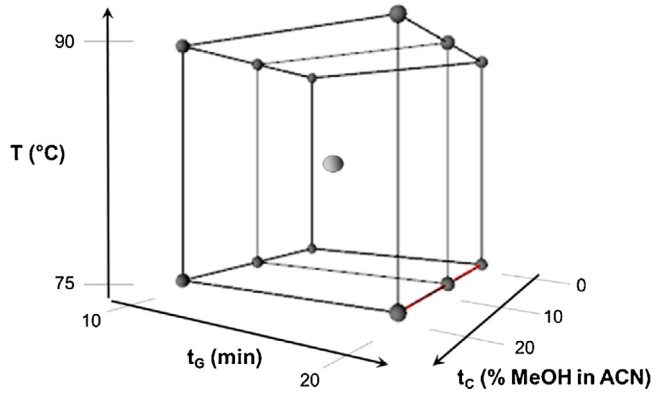

Fig. 4. Suggested experimental design for 3D retention model (column: 150 × 2.1 mm, gradient: 25–50% B at 0.3 mL/min).

species in RPLC. However, these 3 parameters can only be tuned in a limited design space, when considering possible recovery and degradation issues.

3.2. 3D experimental design and retention model

Based on the preliminary studies, a 3D design ($t_G \times T \times tC$ model) was suggested. The levels (and values) of such an experimental design were illustrated on Fig. 4 for a 150 × 2.1 mm column operating at 0.3 mL/min. Several additional preliminary experiments were performed to determine the values of t_G for the initial runs ranging between 4 and 20 min. For most solutes (including proteins), a factor of three was used between the two set levels of t_G, to provide accurate retention modelling (e.g. t_{G1} = 6 min and t_{G2} = 18 min). However, with the ADC subunits analysed in the present study, combining any shorter gradients than 10 min with a longer one (t_G > 15 min) resulted in inaccurate retention model. This is probably due to the very high slope of the LSS model (S) for these large proteins. Finally, it was found that performing t_{G1} = 10 min and t_{G2} = 20 min gradients (difference of a factor two) results in accurate retention modelling and enables the precise prediction of retention times for any gradient program (linear and multilinear too and for extrapolated t_G such as t_G < 10 min).

The experimental data from the twelve experiments were entered into the modelling software. After processing and checking the data accuracy, the retention times of 10 peaks from native ADC and 14 peaks of reduced ADC were matched in each of the chromatograms by using the PeakMatch module of the DryLab software. The peak tracking process was based on peak areas. All the data were automatically transferred into the modelling software but small adjustments for the peak widths were required to get realistic peak capacity in the simulated chromatograms [39]. Please note, that peak tracking based on peak area was not obvious in this work, due to the fact that the sum of the peak areas was expectedly lower at 75 °C *vs.* 90 °C because of the significant on-column adsorption at lower temperature. Some ADC subunits adsorb more intensively onto the stationary phase, while for other peaks (e.g. H3 or L0), the adsorption was less critical. Therefore, peak movements have to be followed and understood before matching the peak areas. Manual adjustment may have to be performed.

After building up the retention model, its accuracy was experimentally verified. Both native and reduced ADC samples were run in the center point of the experimental design. Retention times and chromatograms were also predicted for this condition. Fig. 5 shows the predicted and measured chromatograms and the identification of the 10 and 14 peaks included in the models. As shown in Fig. 5,

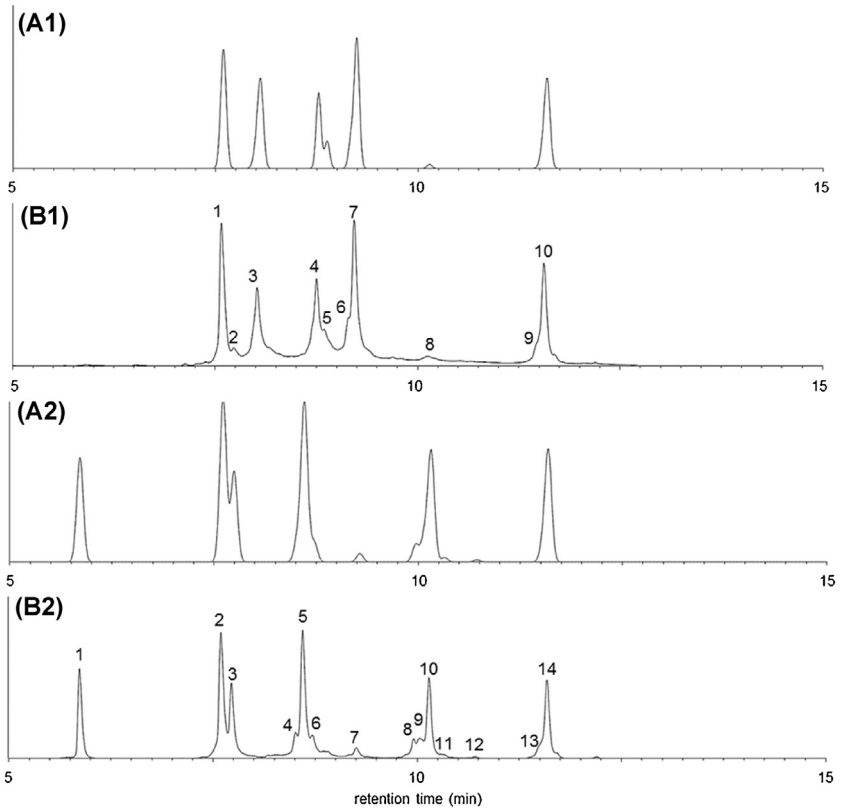

Fig. 5. Model verification in the center point for native Brentuximab vedotin (1) and for reduced Brentuximab vedotin (2). Column: Agilent Advance BioMAb RP C4. Mobile phase "A": 0.1% TFA in water, "B": 0.1% TFA in 90% acetonitrile + 10% MeOH. Flow rate: 0.3 mL/min, gradient: 25–50% B in 15 min, temperature: 82.5 °C, injected volume: 1 μL, detection at 280 nm. "A" corresponds to predicted, while "B" corresponds to experimental chromatograms.

Table 1
Prediction accuracy in the center point of the experimental design for native brentuximab vedotin.

	t_r experimental (min)	t_r predicted (min)	Difference[a]	% error[b]
peak 1	7.575	7.590	−0.01	−0.20
peak 2.	7.726	7.740	−0.01	−0.18
peak 3	8.016	8.050	−0.03	−0.42
peak 4	8.749	8.770	−0.02	−0.24
peak 5	8.844	8.870	−0.03	−0.29
peak 6	9.149	9.170	−0.02	−0.23
peak 7	9.215	9.240	−0.03	−0.27
peak 8	10.124	10.140	−0.02	−0.16
peak 9	11.507	11.530	−0.02	−0.20
peak 10	11.557	11.590	−0.03	−0.28
		average	−0.02	−0.25

[a] Difference = experimental − predicted.
[b] % error = [(experimental − predicted)/predicted] × 100.

the experimentally observed and predicted chromatograms were in very good agreement. Tables 1 and 2 present the difference and % error of measured and calculated retention times for the native and reduced ADC, respectively. There was no more than 0.5% error, and the average error of retention time prediction was below 0.3%.

The verification of the model was assessed by creating resolution maps (Fig. 6). The colour code in these resolution maps represents the value of the critical resolution (Rs), with warm "red" colours corresponding to large resolution values (Rs > 1.0) and cold "blue" colours correspond to low resolution values (Rs < 0.3). The visual inspection of the cubes show the largest red region, where the method is probably robust and the resolutions of all peaks in the chromatogram are the best that can be achieved (when using the initial linear gradient). Based on the resolution cubes, the starting point of the optimization can easily be selected. Further optimization can be done by changing the B% of initial and final mobile phase composition. After changing the B%, again the effect of temperature and ternary composition are worth re-studying. After further optimization, a gradient from 29 to 42%B, with t_G = 14 min at T = 90 °C and tC = 0% MeOH gave a fast and appropriate separation for the native ADC sample (Fig. 7). The experimental verification of this working point again showed high prediction accuracy. The average error of retention time prediction was lower than 0.5%. For the reduced ADC, the optimal conditions were found as a gradient of 31–48%B, t_G = 18 min, T = 90 °C and tC = 20% MeOH (Fig. 8). Similarly, the predicted and experimental chromatograms were in good agreement (lower than 0.5% error).

As illustrated by this example, this generic 3D retention model and optimization for cysteine linked ADCs seems to be interesting. It can also be useful for laboratories working under regulated conditions, since all the possible combinations of method variables can quickly be checked.

The time required for this 12 runs based design and its verification is about 7–8 h for one sample and assuming duplicate injections (2 × (6 × 10 min + 6 × 20 min + 1 × 15 min) + system equilibration). Then the understanding of peak movements, peak tracking, importing chromatograms and creating the model take around 5–6 h. Finally, the optimization and then the experimental verification of the selected working point take an additional 2–3 h of work. In total, this optimization approach of ADC species separations in RPLC mode requires 2–3 working days.

3.3. Simulated robustness testing

An interesting feature of DryLab 4 modelling software is its ability to perform an in-depth "modelled" robustness testing [34]. From the design space, as defined in a resolution cube, it is possible to get robustness information for the measured variables, including t_G, T and tC. The influence of additional parameters, such as flow rate or initial- and final-%B of the gradient, on retention time can be predicted for all compounds. Consequently, the impact of changes in any of these 6 variables/parameters on the resolution can be assessed using a simulated 2^6 or 3^6 type factorial design. After defining the possible deviations from the nominal values, 64 or 729 experiments can be virtually performed. At the end, the software provides a 'frequency distribution graph' showing how often (N) a certain critical resolution occurs under any combination of possible parameters. On the other hand, 'regression coefficients' can also be obtained to show the effect of each parameter, related to the selected deviation from the nominal value, for the critical resolution.

This simulated robustness test was performed around a selected working point as t_G = 27 ± 0.5 min, T = 87 ± 1 °C, tC = 5 ± 1% MeOH, flow rate: 0.30 ± 0.05 mL/min, initial%B: 25 ± 1, final%B: 50 ± 1. This condition allowed the best separation of the L1 and H0 peaks (as critical peak pairs) of the reduced brentuximab vedotin (Fig. 9). The baseline separation of the L0, L1, H0, H1, H2 and H3 species are important for the determination of average DAR. The separation of positional isomers of a given species (e.g. H1 or H2 have 3 different positional isomers) is not mandatory for this purpose. Please note, that the total run time is 27 min but the retention time of the last eluting peak is below 20 min, thus possible thermal degradation is not an issue. Performing the 729 virtual experiments showed that all the experiments met the Rs > 1.5 criterion, thus the conditions defined by our selected working point can be considered as robust (Fig. 9C). The lowest observed resolution was Rs = 1.73 which is still

Table 2
Prediction accuracy in the center point of the experimental design for reduced brentuximab vedotin.

	t_r experimental (min)	t_r predicted (min)	Difference[a]	% error[b]
peak 1	5.868	5.850	0.02	0.31
peak 2.	7.599	7.610	−0.01	−0.14
peak 3	7.729	7.740	−0.01	−0.14
peak 4	8.514	8.520	−0.01	−0.07
peak 5	8.601	8.600	0.00	0.01
peak 6	8.718	8.720	0.00	−0.02
peak 7	9.258	9.280	−0.02	−0.24
peak 8	9.961	9.960	0.00	0.01
peak 9	10.031	10.070	−0.04	−0.39
peak 10	10.148	10.150	0.00	−0.02
peak 11	10.297	10.320	−0.02	−0.22
peak 12	10.711	10.710	0.00	0.01
peak 13	11.543	11.530	0.01	0.11
peak 14	11.592	11.590	0.00	0.02
		average	−0.01	−0.06

[a] Difference = experimental − predicted.
[b] % error = [(experimental − predicted)/predicted] × 100.

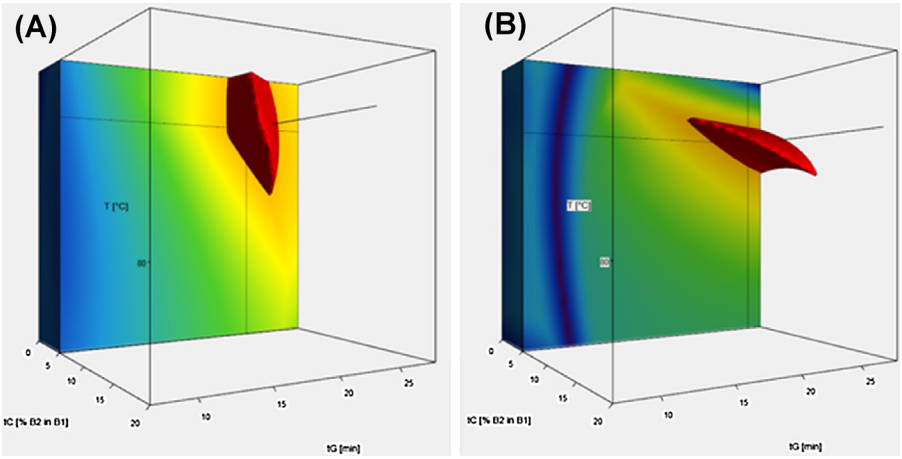

Fig. 6. 3D resolution maps for Brentuximab vadotin (A) and for Brentuximab vedotin reduced (B) samples, based on the initial experiments (Rs crit = 1.0). Set conditions for the native sample: t_G = 23 min, T = 88 °C and tC = 5% MeOH. Set conditions for the reduced sample: t_G = 27 min, T = 87 °C and tC = 5% MeOH. (For interpretation of the references to colour in the text, the reader is referred to the web version of this article.)

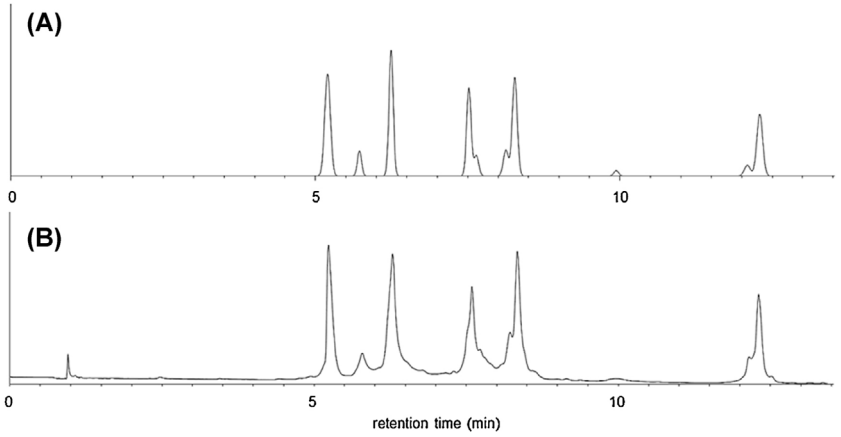

Fig. 7. Predicted (A) and experimentally verified (B) chromatograms of native Brentuximab vedotin under optimal conditions. Gradient: 29–42% B, t_G = 14 min, T = 90 °C and tC = 0% MeOH (100% AcN). (Column: Agilent Advance BioMAb RP C4, flow rate: 0.3 mL/min).

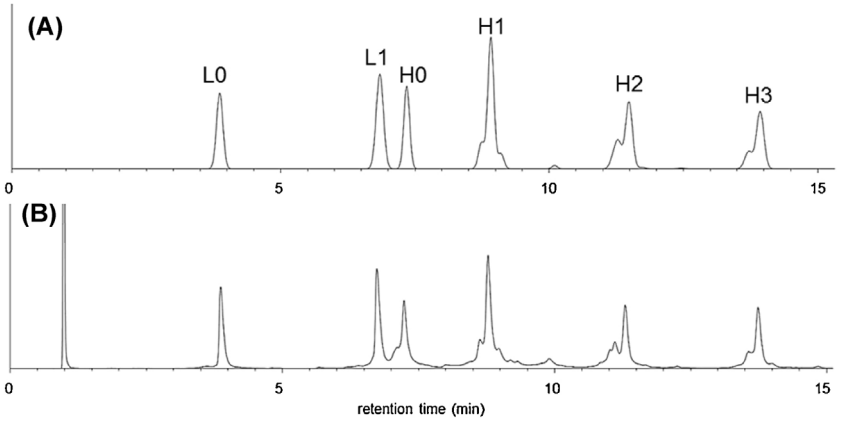

Fig. 8. Predicted (A) and experimentally verified (B) chromatograms of reduced Brentuximab vedotin under optimal conditions to optimize resolution between L1 and H0 species. Gradient: 31–48% B, t_G = 18 min, T = 90 °C and tC = 20% MeOH (80% AcN). (Column: Agilent Advance BioMAb RP C4, flow rate: 0.3 mL/min).

acceptable. The gradient time was found to be the most influential method variable.

Another important fact is that the separation on Fig. 9 takes only 27 min in total while previously a 70 min long RP method was reported for the same sample in Ref. [5]. The gain in analysis time (3 times faster separation) and better separation quality (higher resolution between positional isomers) here is due to the systematic optimization and the understanding of retention behavior.

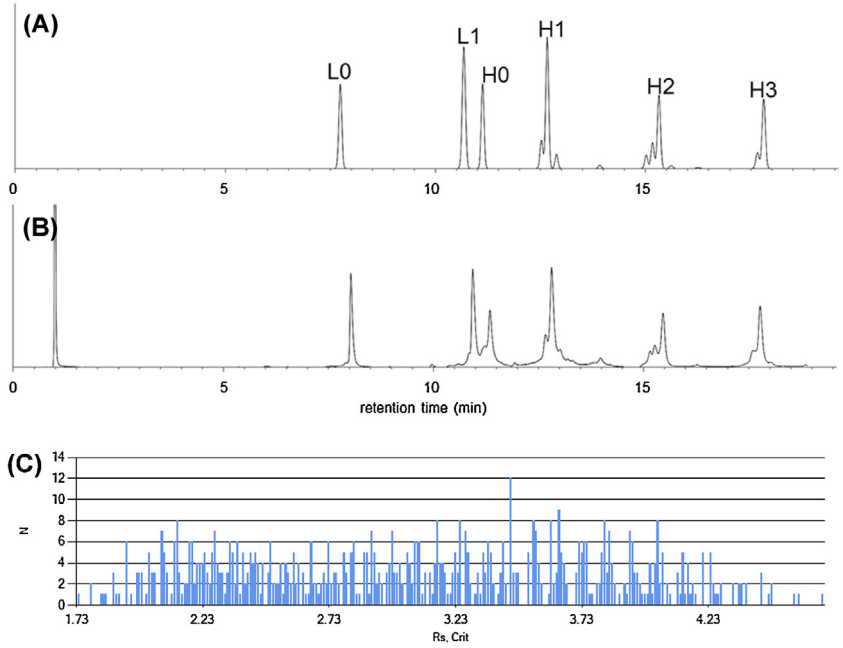

Fig. 9. Predicted (A) and experimentally verified (B) chromatograms of reduced Brentuximab vedotin under optimal conditions to optimize resolution between all peaks. Gradient: 25–50% B, t_G = 27 min, T = 87 °C and tC = 5% MeOH (95% AcN). (Column: Agilent Advance BioMAb RP C4, flow rate: 0.3 mL/min). Panel C represents the result of simulated robustness test as number of observations (N) vs. critical resolution ($R_{s,crit}$).

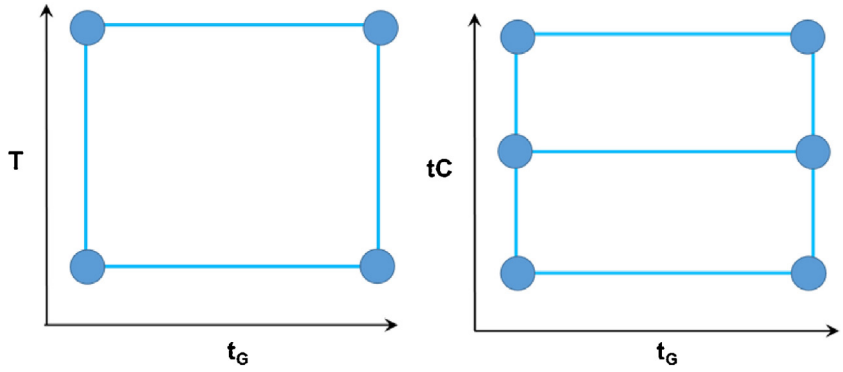

Fig. 10. Simplified 2D experimental designs as t_G x T model (4 runs) and $t_G \times tC$ (6 runs) models.

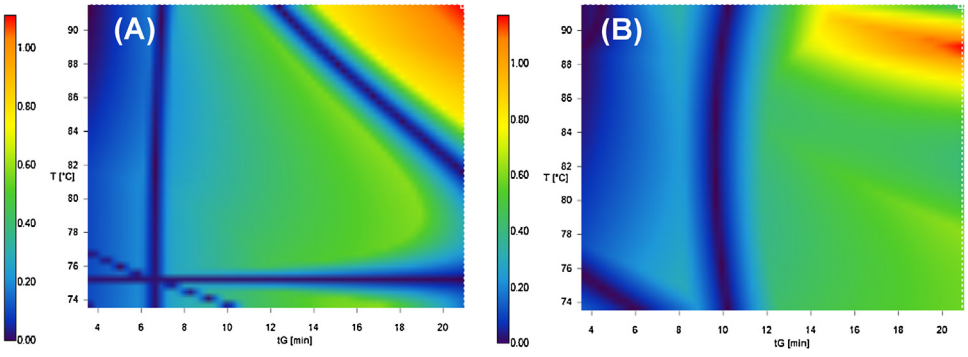

Fig. 11. Simplified 2D resolution maps of native (A) and reduced (B) ADC based on four initial experiments ($t_G \times$ T model). Gradient: 25–50% B, t_{G1} = 10 min, t_{G2} = 20 min, T_1 = 75 °C, T_2 = 90 °C and tC = 0% MeOH (100% AcN). (Column: Agilent Advance BioMAb RP C4, flow rate: 0.3 mL/min).

3.4. Simplified 2D experimental designs

Obviously, the 3D retention model can be simplified to 2D models if required (e.g. to gain in time or if 3D retention modelling software is not available). One possibility is to select a $t_G \times$ T model which requires four initial runs, while the other choice is to perform a $t_G \times tC$ model which necessitates six experiments (Fig. 10).

To perform a $t_G \times$ T model, ternary mobile phase composition is not suggested. Since the best recovery was obtained with ACN, the mobile phase B should preferably be 0.1% TFA in ACN as a

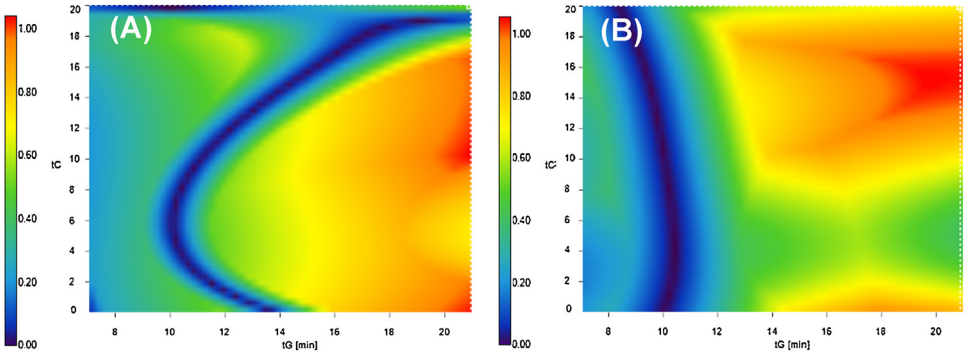

Fig. 12. Simplified 2D resolution maps of native (A) and reduced (B) ADC based on six initial experiments ($t_G \times tC$ model). Gradient: 25–50% B, t_{G1} = 10 min, t_{G2} = 20 min, tC_1 = 0% MeOH, tC_2 = 10% MeOH and tC_3 = 20% MeOH, T = 90 °C. (Column: Agilent Advance BioMAb RP C4, flow rate: 0.3 mL/min).

first choice. The time required for the experiments is only around 2–3 h (2 × (2 × 10 min + 2 × 20 min) + system equilibration) for one sample (with duplicate injections). Fig. 11 shows the obtained 2D resolution maps for the native and reduced ADC. The blue lines indicate co-elutions (and therefore elution order changes). Since the blue lines oriented in both vertical and horizontal directions on the map, the design space indeed seems to be well selected since both method variables play an important role in the overall quality of the separation.

Fig. 12 shows the obtained 2D resolution maps for a $t_G \times tC$ model. In this case, the temperature should be set as high as possible to avoid recovery issues (e.g. T = 90 °C). This experimental design takes around 3–4 h of work (2 × (3 × 10 min + 3 × 20 min) + system equilibration). The maps again suggest that both variable (t_G and tC) have a huge impact on the critical resolution and therefore makes this model interesting for routine applications.

Both 2D models provided similar maximum resolution and analysis time as for an optimal method. If further optimization is required then the $t_G \times$ T model can be repeated with a ternary mobile phase (e.g. 20% MeOH + 80% ACN as organic solvent) while the $t_G \times tC$ model can be performed again, but at a different temperature (e.g. at 80 °C). This repeated experiments may perform better quality of separation. If it is not the case, then the best choice is to perform one of these 2D models on a different stationary phase.

3.5. Determination of the average DAR

One method of choice to determine the average DAR of an ADC is based on the observed peak area ratios of RPLC chromatogram of the reduced ADC:

$$DAR = 2x\left(\sum_{i=0}^{1} weighted\ peak\ area\ of\ L(i) + \sum_{i=0}^{3} weighted\ peak\ area\ of\ H(i)\right)/100$$

Both optimum conditions (presented in Figs. 8 and 9) resulted in DAR = 4.0. This value is in good agreement with those reported in the literature [6,7,17]. However, it is worth mentioning that the average DAR was calculated for all the initial runs (at 75 and 90 °C), and we systematically observed larger DAR value (as DAR = 4.2–4.3) at 75 °C compared to 90 °C (DAR = 4.0). Finally, this is not surprising since the poorer recovery of some species results in differences in pear area% distribution. Logically, the DAR determined at lower temperature is not correct, and therefore attention should be paid when calculating the average DAR from RPLC chromatograms.

4. Conclusions

A new 3D retention model was suggested and successfully applied in RPLC for IgG1 cysteine conjugated antibody drug conjugate (ADC). In total, the optimization of this 3D retention model required only 2–3 working days (12 experiments for one sample). In addition to the 3D model, simplified 2D models could also be done for fast method development which took less than one day (4 or 6 experiments with one sample). Generic (platform) method development approach was found to be feasible. The time saving of this systematic methodology is obvious compared to trial and error approach.

The most important method variables to optimize ADC separation were the gradient steepness (1), mobile phase temperature (2) and mobile phase ternary composition (3). The retention time prediction offered by the retention models was found to be highly accurate, with an average error lower than 0.5%.

The developed RPLC method can be considered for determining the average DAR of an ADC, based on the observed peak area ratios of the reduced ADC sample. The native ADC separation can also be useful for multidimensional separations in the second dimension to separate the positional isomers and different species and enabling the MS identification.

It also worth mentioning that – by understanding the retention behavior of ADC peaks – analysis time could be shortened into the 20–25 min range while 60–70 min long separations were reported previously.

Acknowledgements

The authors wish to thank Alain Beck from Pierre Fabre for providing the antibody drug conjugate sample.

Davy Guillarme wishes to thank the Swiss National Science Foundation for support through a fellowship to Szabolcs Fekete (31003A 159494).

References

[1] R.V.J. Chari, Targeted cancer therapy: conferring specificity to cytotoxic drugs, Acc. Chem. Res. 41 (2008) 98–107.
[2] S. Ornes, Antribody drug conjugates, Proc. Natl. Acad. Sci. U. S. A. 110 (2013) 13695.
[3] A. Wakankar, Y. Chen, Y. Gokarn, F.S. Jacobson, Analytical methods for physicochemical characterization of antibody drug conjugates, mAbs 3 (2011) 161–172.
[4] B. Wiggins, L. Liu-Shin, H. Yamaguchi, G. Ratnaswamy, Characterization of cysteine-linked conjugation profiles of immunoglobulin G1 and immunoglobulin G2 antibody–drug conjugates, Pharm. Drug Deliv. Pharm. Tech. 104 (2015) 1362–1372.
[5] L.N. Le, J.M. Moore, J. Ouyang, X. Chen, M.D. Nguyen, W.J. Galush, Profiling antibody drug conjugate positional isomers: a system of-equations approach, Anal. Chem. 84 (2012) 7479–7486.

[6] S. Heinisch, M. Sarrut, D. Guillarme, A. Beck, S. Fekete, M.C.J. Bussat, O. Colas, Analysis of antibody-drug conjugates by comprehensive on-line two-dimensional hydrophobic interaction chromatography x reversed phase liquid chromatography hyphenated to high resolution mass spectrometry. II – identification of sub-units for the characterization of even and odd load drug species, J. Chromatogr. B 1032 (2016) 91–102.
[7] M. Sarrut, A. Corgier, S. Fekete, D. Guillarme, D. Lascoux, M.C.J. Bussat, A. Beck, S. Heinisch, Analysis of antibody-drug conjugates by comprehensive on-line two-dimensional hydrophobic interaction chromatography x reversed phase liquid chromatography hyphenated to high resolution mass spectrometry. I – optimization of conditions, J. Chromatogr. B 1032 (2016) 103–111.
[8] B.C. Laguzza, C.L. Nichols, S.L. Briggs, G.J. Cullinan, D.A. Johnson, J.J. Starling, New antitumor monoclonal antibody-vinca conjugates LY203725 and related compounds: design, preparation and representative in vivo activity, J. Med. Chem. 32 (1989) 548–555.
[9] R.V. Chari, B.A. Martell, J.L. Gross, S.B. Cook, S.A. Shah, W.A. Blattler, Immunoconjugates containing novel maytansinoids: promising anticancer drugs, Cancer Res. 52 (1992) 27–31.
[10] F. Hudecz, M.C. Garnett, T. Khan, R.W. Baldwin, The influence of synthetic conditions on the stability of methotrexate-monoclonal antibody conjugates determined by reversed phase high performance liquid chromatography, Biomed. Chromatogr. 6 (1992) 128–132.
[11] R.V. Chari, K.A. Jackel, L.A. Bourret, S.M. Derr, B.M. Tadayoni, K.M. Mattocks, Enhancement of the selectivity and antitumor efficacy of a CC-1065 analogue through immunoconjugate formation, Cancer Res. 55 (1995) 4079–4084.
[12] R.S. Greenfield, T. Kaneko, A. Daues, M.A. Edson, K.A. Fitzgerald, L.J. Olech, Evaluation in vitro of adriamycin immunoconjugates synthesized using an acid-sensitive hydrazone linker, Cancer Res. 50 (1990) 6600–6607.
[13] D. Willner, P.A. Trail, S.J. Hofstead, H.D. King, S.J. Lasch, G.R. Braslawsky, (6-maleimidocaproyl)hydrazone of doxorubicin, a new derivative for the preparation of immunoconjugates of doxorubicin, Bioconjugate Chem. 4 (1993) 521–527.
[14] M.M. Sun, K.S. Beam, C.G. Cerveny, K.J. Hamblett, R.S. Blackmore, M.Y. Torgov, Reduction-alkylation strategies for the modification of specific monoclonal antibody disulfides, Bioconjugate. Chem. 16 (2005) 1282–1290.
[15] C.F. McDonagh, E. Turcott, L. Westendorf, J.B. Webster, S.C. Alley, K. Kim, Engineered antibody-drug conjugates with defined sites and stoichiometries of drug attachment, Protein Eng. Des. Sel. 19 (2006) 299–307.
[16] K.J. Hamblett, P.D. Senter, D.F. Chace, M.M. Sun, J. Lenox, C.G. Cerveny, Effects of drug loading on the antitumor activity of a monoclonal antibody drug conjugate, Clin. Cancer Res. 10 (2004) 7063–7070.
[17] B. Bobaly, A. Beck, J.L. Veuthey, D. Guillarme, S. Fekete, Impact of organic modifier and temperature on protein denaturation in hydrophobic interaction chromatography, J. Pharm. Biomed. Anal. 131 (2016) 124–132.
[18] S. Fekete, J.L. Veuthey, A. Beck, D. Guillarme, Hydrophobic interaction chromatography for the characterization of monoclonal antibodies and related products, J. Pharm. Biomed. Anal. 130 (2016) 3–18.
[19] A. Cusumano, D. Guillarme, A. Beck, S. Fekete, Practical method development for the separation of monoclonal antibodies and antibody-drug-conjugate species in hydrophobic interaction chromatoraphy, part 2: optimization of the phase system, J. Pharm. Biomed. Anal. 121 (2016) 161–173.
[20] M.M. Siegel, I.J. Hollander, P.R. Hamann, J.P. James, L. Hinman, B.J. Smith, Matrix-assisted UV-laser desorption/ionization mass spectrometric analysis of monoclonal antibodies for the determination of carbohydrate, conjugated chelator and conjugated drug content, Anal. Chem. 63 (1991) 2470–2481.
[21] J.R. Junutula, K.M. Flagella, R.A. Graham, K.L. Parsons, E. Ha, H. Raab, Engineered thio-trastuzumab-DM1 conjugate with an improved therapeutic index to target human epidermal growth factor receptor 2-positive breast cancer, Clin. Cancer Res. 16 (2010) 4769–4778.
[22] L. Wang, G. Amphlett, W.A. Blattler, J.M. Lambert, W. Zhang, Structural characterization of the maytansinoid-monoclonal antibody immunoconjugate huN901-DM1, by mass spectrometry, Protein Sci. 14 (2005) 2436–2446.
[23] A.C. Lazar, L. Wang, W.A. Blattler, G. Amphlett, J.M. Lambert, W. Zhang, Analysis of the composition of immunoconjugates using size-exclusion chromatography coupled to mass spectrometry, Rapid Commun. Mass Spectrom. 19 (2005) 1806–1814.
[24] M.C. Janin Bussat, M. Dillenbourg, N. Corvaia, A. Beck, C. Klinguer-Hamour, Characterization of antibody drug conjugate positional isomers at cysteine residues by peptide mapping LC–MS analysis, J. Chromatogr. B 981–982 (2015) 9–13.
[25] T. Chen, Y. Chen, C. Stella, C.D. Medley, J.A. Gruenhagen, K. Zhang, Antibody-drug conjugate characterization by chromatographic andelectrophoretic techniques, J. Chromatogr. B 1032 (2016) 39–50.
[26] S. Fekete, S. Rudaz, J. Fekete, D. Guillarme, Analysis of recombinant monoclonal antibodies by RPLC: towards a generic method development approach, J. Pharm. Biomed. Anal. 70 (2012) 158–168.
[27] S. Fekete, S. Rudaz, J.L. Veuthey, D. Guillarme, Impact of mobile phase temperature on recovery and stability of monoclonal antibodies using recent reversed-phase stationary phases, J. Sep. Sci. 35 (2012) 3113–3123.
[28] J.A. Lewis, L.R. Snyder, J.W. Dolan, Initial experiments in high-performance liquid chromatographic method development II. Recommended approach and conditions for isocratic separation, J. Chromatogr. A 721 (1996) 15–29.
[29] J.W. Dolan, L.R. Snyder, N.M. Djordjevic, D.W. Hill, D.L. Saunders, L. Van Heukelem, T.J. Waeghe, Simultaneous variation of temperature and gradient steepness for reversed-phase high-performance liquid chromatography method development: I. Application to 14 different samples using computer simulation, J. Chromatogr. A 803 (1998) 1–31.
[30] L.R. Snyder, J.J. Kirkland, J.L. Glajch, Practical HPLC Method Development, second ed., John Wiley & Sons Inc., 1997.
[31] J.C. Berridge, Techniques for the Automated Optimization of HPLC Separations, John Wiley & Sons, New York, 1986.
[32] R. Kormány, I. Molnár, H.J. Rieger, Exploring better column selectivity choices in ultra-high performance liquid chromatography using Quality by Design principles, J. Pharm. Biomed. Anal. 80 (2013) 79–88.
[33] N. Rácz, R. Kormány, J. Fekete, I. Molnár, Establishing column batch repeatability according to Quality by Design (QbD) principles using modeling software, J. Pharm. Biomed. Anal. 108 (2015) 1–10.
[34] R. Kormány, J. Fekete, D. Guillarme, S. Fekete, Reliability of simulated robustness testing in fast liquid chromatography using state-of-the-art column technology, instrumentation and modelling software, J. Pharm. Biomed. Anal. 89 (2014) 67–75.
[35] Y. Chen, C.T. Mant, R.S. Hodges, Temperature selectivity effects in reversed-phase liquid chromatography due to conformation differences between helical and non-helical peptides, J. Chromatogr. A 1010 (2003) 45–61.
[36] C.T. Mant, Y. Chen, R.S. Hodges, Temperature profiling of polypeptides in reversed-phase liquid chromatography: I. Monitoring of dimerization and unfolding of amphipathic α-helical peptides, J. Chromatogr. A 1009 (2003) 29–43.
[37] C.T. Mant, B. Tripet, R.S. Hodges, Temperature profiling of polypeptides in reversed-phase liquid chromatography: II. Monitoring of folding and stability of two-stranded α-helical coiled-coils, J. Chromatogr. A 1009 (2003) 45–59.
[38] S. Fekete, A. Beck, E. Wagner, K. Vuignier, D. Guillarme, Adsorption and recovery issues of recombinant monoclonal antibodies in reversed-phase liquid chromatography, J. Sep. Sci. 38 (2015) 1–8.
[39] A.H. Schmidt, I. Molnár, Using an innovative Quality-by-Design approach for development of a stability indicating UHPLC method for ebastine in the API and pharmaceutical formulations, J. Pharm. Biomed. Anal. 78-79 (2013) 65–74.